ILASS–Europe 2022, 31th Conference on Liquid Atomization and Spray Systems, 6-8 September 2022, Virtual

Nucleation and Bubble Growth in a Rapidly Heated Composite Drop

Tali Bar-Kohany*[1,2], Dmitrii V. Antonov, Pavel A. Strizhak[3], Sergei S. Sazhin[4]

[1]School of Mechanical Engineering, Tel Aviv University, Tel Aviv, Israel
[2]Department of Mechanical Engineering, nrcn, Israel
[3]National Research Tomsk Polytechnic University 30, Lenin Avenue, Tomsk 634050, Russia
[4]Advanced Engineering Centre, School of Architecture, Technology and Engineering, University of Brighton, Brighton, BN2 4GJ, UK

*Corresponding author: talibk@tauex.tau.ac.il

Abstract
Nucleation occurs when liquid is heated to temperature above its saturation temperature. In the present paper, we examine theoretically the effect of rapid heating on the nucleation and bubble growth in a composite drop. In the general case bubble growth rate is dominated by superheating degree and growth time is dominated by relative location of the bubble with respect to the inner and outer interfaces of the composite drop. Nucleation location, either completely within the inner drop (sub-drop) or at the interface (bubble blowing) controls the size that the bubble which is expected to grow to reach the outer interface and hence important to the growth time before breakup. The model for puffing and micro-explosion presented in the paper considers an isolated bubble growing at the water/fuel interface and at the centre of the water sub-drop at various superheating degrees. This analysis will allow us to assess the sensitivity of bubble growth time to the initial bubble location, and to generalise the previously developed model of the phenomenon taking into account the effect of finite time of bubble growth during the development of puffing/micro-explosion.

Keywords
Nucleation, Rapid Heating, Bubble Growth, Composite Drop, Micro-Explosion, Puffing.

Introduction

Puffing and Micro-Explosions (ME) in composite drops are gaining popularity in engineering applications, mainly to promote more efficient, and thus cleaner combustion or to extinguish flames. In diesel engines, for example, other methods like EGR (Exhaust Gas Recirculation) or oxygen enrichment are used. However, while EGR reduces NO_x it promotes particulates formation, O_2 enrichment does exactly the opposite. Emulsified fuel, in-contrast, reduces both NO_x and particulates, and increases combustion efficiency by enhancing mixing due to puffing/ME.

The aim of this study to investigate the effect of heating rate on initiation of nucleation and bubble growth in a rapidly heated composite drop. In previous papers [1] [2] [3], the impact of heating rate on the time to puffing/ME without taking into account its effect on the bubble growth period was considered. Composite fuel drops do not undergo any special treatment and therefore it is reasonable to assume that nucleation centres, in the form of suspensions or colloids, are present within them. In addition, when PLIF (Planar Laser-Induced Fluorescence) measurements are used, nucleation centres are always present. For example, micron-sized organic dye particles (Rhodamine B) were used in the previous studies to measure the interface temperature, along with a Phantom HSV (High-Speed Video) [1] [2] [4]. In the nucleation centres (ready-centres) lower energy barrier is required for the formation of

a new phase, and thus heterogeneous nucleation (HtN) rather than homogeneous nucleation (HN) is expected to take place.
The heating rate determines the heterogeneous nucleation temperature of a given liquid (see **Figure 1** and Equations (1)-(3) for water at atmospheric pressure, adapted from [1]).

$$T_N = T_{sat}\left(1 + 0.37\,\dot{T}^{10/626}\right) \quad \text{when} \quad 10^{5.5} \le \dot{T} \le 10^{9}\ K/S. \tag{1}$$

$$T_N = 385 + 160\,tanh\left(\dot{T}/10^{5}\right) \quad \text{when} \quad 10^{2} \le \dot{T} \le 10^{5.5}\ K/S. \tag{2}$$

$$T_N = T_{sat} + 12\,tanh\left(\dot{T}/50\right) \quad \text{when} \quad 0 \le \dot{T} \le 300\ K/S. \tag{3}$$

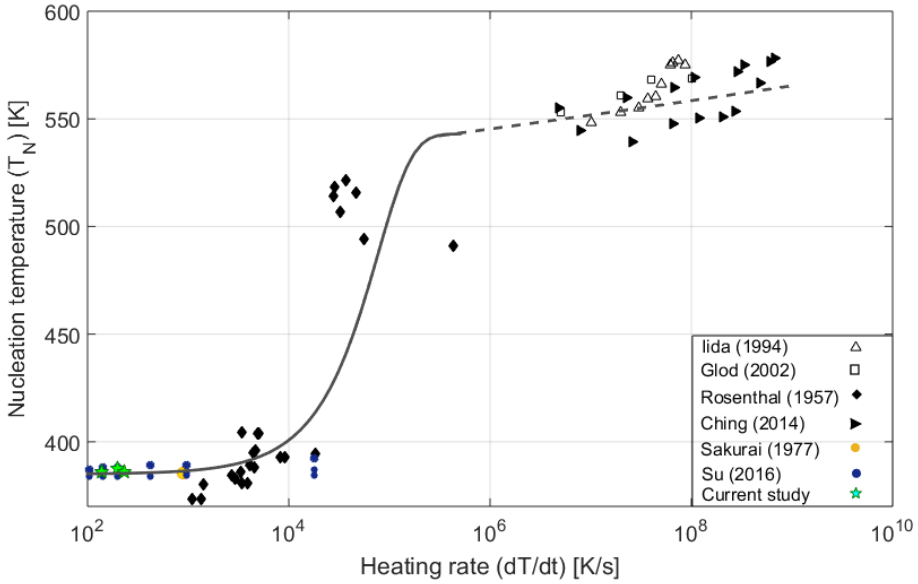

Figure 1. Nucleation temperature T_N versus heating rate $\dot{T}$ =*dT/dt* – a comparison between prediction by Expressions (1) (dashed) and (2) (solid), and experimental data obtained in [5] (Current study), and six other groups (references are given in [1]). Reprinted from [1], Copyright Elsevier (2020).

Once the interface temperature (T_w, black thick solid curve in Figure **2**) reached the nucleation temperature (T_N, black dashed-dotted curve in Figure **2**), it was assumed that nucleation occurs. The case of n-dodecane/water drops with initial radii and temperature equal to 5 μm and 300 K, respectively, and with the volume fraction of water equal to 15%, placed in gas at atmospheric pressure and temperature 700 K is shown in this figure. As follows from **Figure 2**, the time to puffing/ME increases three-fold by considering the nucleation temperature rather than saturation (boiling) temperature, from about 0.135 ms to about 0.41 ms.
Once a thermodynamically stable bubble incepts (the change in its Gibbs energy reaches a maximal value with respect to the vapour embryo's radius at the nucleation temperature ([6] [7]), its growth process ensues. The growth rate is determined by superheat degree, which is the temperature difference between the nucleation and saturation temperature ($\Delta T_{SH} = T_N - T_{sat}$). The former, as mentioned earlier, is controlled by the heating rate and the number density of existing ready-centres.

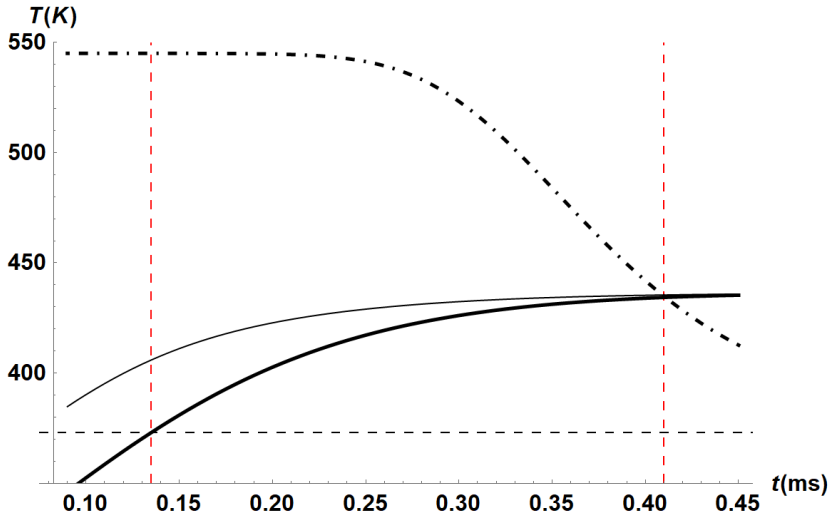

Figure 2. The plots of time evolution of T_w (thick solid), T_s (thin solid), T_N (dashed-dotted) and T_B (horizontal dashed line); the vertical dashed lines show the time instant when $T_w = T_{sat}$ and $T_w = T_N$. Reprinted from [1], Copyright Elsevier (2020).

An increase in the superheating degree implies larger driving force for the bubble growth. The bubble growth process can be divided into three regimes [8], each being limited by a different physical phenomenon: surface-tension, inertial and heat transfer controlled. The surface tension-controlled regime is basically the appearance of a stable vapour nucleon. In most cases, the inertial regime, where the bubble radius is a linear function of time, can be ignored. The dominant regime during the later stages of the bubble growth process is the heat-transfer regime. According to the classical model, the bubble radius growth during this regime can be evaluated as [10]:

$$R_b = 2\,C_r\sqrt{\alpha_f t_{gr}}; \quad C_r = Ja\sqrt{3/\pi}, \tag{4}$$

$$Ja \equiv \frac{\rho_f}{\rho_g}\frac{C_{p,f}\,\Delta T_{SH}}{h_{fg}}, \tag{5}$$

Ja is the Jakob number, which represents the ratio between the sensible to latent heat, and t_{gr} is the growth period of the bubble.

In the present paper, we will examine the effect of the use of different bubble growth models on the time to puffing/ME by comparing the classical model to Zanje et al. correlations, stemming from their numerical model [11]. The latter was shown to be more accurate than the classical one for a wide range of *Ja*.

The non-dimensional bubble radius (R_b^+) and time of growth (t^+) that are appropriate for both Mikic et al. and Zanje et al. models are:

$$R_b^+ = \frac{A}{B^2}R_b\,; \quad t^+ = \frac{A^2}{B^2}t_{gr} \tag{6}$$

$$A = \sqrt{\frac{2}{3}\frac{\rho_f}{\rho_g}\frac{h_{fg}\,\Delta T_{SH}}{T_{sat}}}\,; \quad B = Ja\sqrt{\frac{12}{\pi}\alpha_f} \tag{7}$$

The time at which the puffing/ME event takes place (droplet breakup time, t_{br}) is comprised of three main contributions: heating (nucleation, t_N), bubbles' growth (t_{gr}) and oscillations (t_{osc}):

$$t_{br} = t_N + t_{gr} + t_{osc} \quad (8)$$

In the present study, we will address only the first two contributions for single, stationary composite drops of various sizes. Stavros et al. [12] assumed that the emulsion-induced breakup time can be split into the heating and bubble growth time periods. They studied numerically a single composite drop representing drops moving in a spray with relative velocities ranging from 40 m/s to 100 m/s at various ambient temperatures and pressures. The outer fuel drop diameter was 50 μm and the inner water drop diameter varied from 0.1 μm to 24 μm. They assumed that the nucleation temperature equals the homogeneous nucleation temperature, and thus found that oscillations might be provoked (see [13] for the case in a pure drop) due to the growth of a bubble within the liquid drop.

Results and Discussion

The size of the bubbles at the time instant when puffing/ME starts (t_{br}, not to be confused with the nucleation time, t_N) is mainly determined by its relative location with respect to the outer boundary. This is also influenced by the relative location of the inner drop. In the previous study [2], we found that for a water/diesel fuel mixture the inception of the bubble occurs at the W/F interface via the bubble blowing mechanism for mixtures containing mass fractions of water below ~50% for bulk temperatures higher than 20°C. We assume that the models for a single bubble formed in an infinite domain are applicable to our case. For both cases, either the bubble is initiated at the centre of the inner (water) drop, or at the W/F interface, the breakup occurs when the bubble reaches the outer surface. For the case where the bubble is initiated at interface (bubble blowing) we assume that the maximal size of the bubble is equal to the minimal gap between the inner and the outer drops ($R_{b,max} = R_s - R_w$). For the case where the bubble is initiated at the centre of water drop, we assume that the maximal size of the bubble is equal to the fuel drop radius (R_s). We assume that in case of asymmetry in the location of the inner drop, it is more likely that the bubble will reach the outer boundary where the distance between the boundaries is narrower.

For the case presented in **Figure 2** (dT/dt = 3.15·10^4 K/s, T_N = 434 K, Ja = 182, and the initial outer radius is 5 μm) the heating time is dominant until the breakup event ($t_e \approx t_N$ = 0.41 ms) and the bubble growth time is negligible (<1 μs, see **Figure 3**). This is due to the narrow gap between the two boundaries, which is of the order of microns, and thus the bubble growth time (t_{gr}) is of the order of microseconds. It is worth noting that for these extremely short growth times, there is a notable difference between the classic model by Mikic et al. [17] and the model by Zanje et al. [11]. The latter developed a numerical model to account for all growth regimes for a wide range of Jakob numbers. **Figure 4** presents the Zanje et al. [11] provided correlations to fit all regimes. It appears that the predictions of two models coincide only for the heat transfer regime. The inertial regime according to Zanje et al. ends at 0.15 μs, and the heat transfer regime starts at 0.94 μs. Thus, for the drop under consideration, the intermediate regime is dominant. Note that the growth time predicted by both models for this drop is shorter than 1 μs and compared to the heating time of a stationary drop in that case (0.41 ms) it is certainly of minor importance.

For the same drop size, increasing the heating rate will shorten the heating time significantly. For example, a constant heating rate of 10^7 K/s will result in a higher nucleation temperature and Jakob number (T_N = 551.8 K, Ja = 534) and at the same time in a shorter heating time (t_N =2.6 μs). In this case a bubble growth time becomes very important when estimating the duration of the entire breakup process. Moreover, the differences between the predictions of

these models become very significant; 0.24 μs (9% of the total breaking time) predicted by the Mikic et al. model versus 0.95 μs (27% of the total breaking time) predicted by the Zanje et al. model.

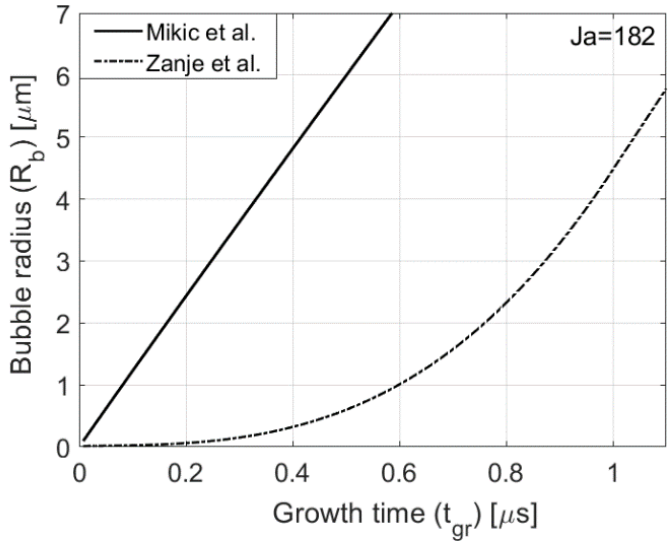

Figure 3. Bubble radius vs. growth time (see Expressions (5) and (6)) for *Ja*=182 evaluated using two models: Zanje et al.[11] and Mikic et al. [17].

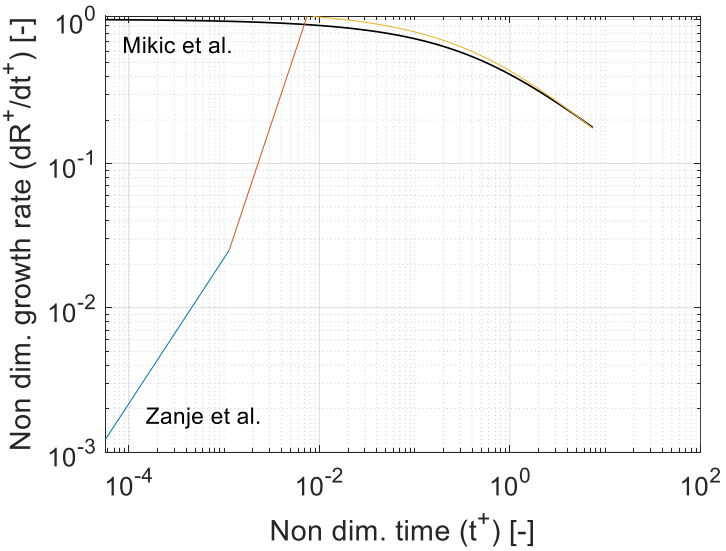

Figure 4. Non-dimensional growth rate vs. non-dimensional growth time for *Ja*=182, evaluated using two models: blue, orange & yellow curves - Zanje et al.[11] and black curve – Mikic et al. [17].

For the same heating rate and nucleation temperature (dT/dt = 3.15·10^4 K/s, T_N = 434 K), for a 1 mm drop, the growth time becomes more significant (~0.12 ms), compared to the heating time (until nucleation at t_N~3 ms). Yet, even for that case, the heating time is dominant over the bubble growth time. It is worth noting that for these timescales, the difference between the predictions of two models is insignificant. In that case the heat transfer regime is the dominant regime.

Conclusions

Higher nucleation temperature trails faster bubble growth rates due to higher superheating degree. This may lead to faster occurrence of puffing/ME. Faster heating rates trail higher nucleation temperatures that imply higher Jakob numbers and larger driving forces for bubbles' growth. This, along with the effect on the time to nucleation, and hence the bubble growth duration, may affect the size of the bubbles. The latter will eventually cause puffing and micro-explosions, and subsequently the secondary drop formation by puffing/ME.

Bubble growth rate is determined by the superheat degree (SH), while its growth time and the bubble size at the time instant when puffing/ME starts are mainly determined by the relative location of the inner drop and the relative location of the bubble with respect to the outer boundary. This is because the puffing/ME event occurs when the bubble reaches the outer boundary of the composite drop.

In most cases for composite drops of water/n-dodecane, nucleation incepts at the inner interface via the bubble blowing mechanism. In the present analysis we assume that puffing/ME events occur once the bubble's size is equal to that of the minimal gap between the outer and inner boundaries. It was shown that the heating duration is dominant over the growth duration for slow to moderate heating rates that lead to low to intermediate nucleation temperatures. However, when the heating rate increases the contribution of the bubble growth period becomes significant.

Acknowledgments

The authors are grateful for the financial support received from the National Research Tomsk Polytechnic University (Priority-2030-NIP/EB-006-0000-2022) which supported D.V. Antonov and P.A. Strizhak (who contributed to the preparation of the experiments and the analysis of the results) and S. S. Sazhin (who contributed to the analysis of the results and preparation of the text of the paper).

Nomenclature

C_p	specific heat capacity [J/kg-K]
h	enthalpy [J/kg]
Ja	Jakob number [-]
R	bubble radius [m]
T	temperature [K]
$\dot{T}$	heating rate [K/s]
t	time [s]

Greek symbols

α	thermal diffusivity [m^2/s]
Δ	difference [-]
ρ	density [kg/m^3]
σ	surface tension [N/m]

Superscripts

+	Non-Dimensional

Subscripts

b	bubble
br	*breakup*
i	interface
F	fuel
f	saturated liquid
g	saturated vapour
gr	growth
max	maximal
N	nucleation
ONB	Onset of Nucleate Boiling
SH	superheated
s	surface
sat	saturation
W	water
w	water/fuel interface

References

[1] Sazhin, S.S., Bar-Kohany, T., Nissar, Z., Antonov, D., Strizhak, P.A., 2020, Int. J of Heat Mass Transfer, 161, 120238.
[2] Bar-Kohany, T., Antonov, D., Strizhak, P.A., Sazhin S.S., Aug. 30 - Sept. 2., 2021, 15th ICLASS, International Conference on Liquid Atomization and Spray Systems, paper 19.
[3] Sazhin, S.S., Bar-Kohany, T., Antonov, D., Strizhak, P.A., 2022, Proceedings of 10th ISFEH, International Seminar on Fire and Explosion Hazards (Oslo, May 22-27, 2022).
[4] Kuznetsov, G.V., Piskunov, M.V., Volkov, R.S., and Strizahk P.A., 2018, Applied Thermal Engineering, 131, pp. 340-355.
[5] Sazhin, S.S., Rybdylova, O.D., Crua, C., Heikal, M., Ismael, M.A., Nissar, Z., Aziz, A.R.B.A., 2019, Int. J of Heat Mass Transfer, 131, pp. 815-821.
[6] Bar-Kohany, T., Amsalem, Y., 2018, Int. J of Heat and Mass Transfer, 126, pp. 411-415.
[7] Carey, V.P, 2020, "Liquid-Vapor Phase-Change Phenomena", CRC Press.
[8] Bar-Kohany, T., Levy, M., 2016, Atomization and Sprays, 26, pp. 1259-1305.
[9] Avulapati M.M., Megaritis, T., Xia, J., and Ganippa, L., 2019, Fuel, 239, pp.1284-1292.
[10] Plesset, M.S., Zwik, S.A., 1954, J. Applied Physics, 25, pp. 493-500.
[11] Zanje, S., Iyer, K., Murallidharan, J. S., Punekar, H., & Gupta, V. K., 2021, Physics of Fluids, 33, 077116.
[12] Stavros, F., Strotos, G., Nikolopoulos, N., and Gavaises, M., 2021, Int. J of Heat and Mass Transfer, 164, 120581.
[13] Shepherd, J. E., Sturtevant, B., 1982, J Fluid Mechanics, 121, pp. 379-402.
[14] Girin, O.G., 2017, Atomization and Sprays, 27, pp.407-422.
[15] Shinjo, J., Xia, L.C., Ganippa, L.C, and Megaritis, A., 2014, Physics of Fluids, 26, 103302.
[16] Yi, P. Li, T., Fu, Y., and Xie, S., 2021, Fuel, 284, 118892
[17] Mikic, B.B., Rohsenow, W.M., Griffith, P., 1970, Int. J of Heat Mass Transfer, 13, pp. 657-666.